Colloids and Surfaces B: Biointerfaces 201 (2021) 111620

Contents lists available at ScienceDirect

Colloids and Surfaces B: Biointerfaces

journal homepage: www.elsevier.com/locate/colsurfb

Chemoselective ligation assisted DNA walker for analysis of double targets

Tianxiang Xue [a], Longfei Tang [a], Xiquan Yue [a], Lili Niu [a], Jinhui Peng [b,*], Juan Zhang [a,*]

[a] Center for Molecular Recognition and Biosensing, School of Life Sciences, Shanghai University, Shanghai, 200444, China
[b] Department of Joint Surgery and Orthopedic Medicine, Shanghai Changzheng Hospital, Second Military Medical University, Shanghai, 200003, China

ARTICLE INFO

Keywords:
Chemoselective ligation
DNA walker
Dual analysis
Double targets

ABSTRACT

Chemoselective ligation assisted DNA walker with input and output of double signals, has been constructed through simultaneous assistance of oxime chemistry and alkyne-azide cycloaddition. The constructed DNA walker has been further developed as a biosensor with lipopolysaccharide (LPS) and 5-hydroxymethyl-2-furaldehyde (HMF) as targets. The biosensor owns one-to-one mapping functionality and can sensitively distinguish all cases of two targets through the unique output signal feature. Moreover, the biosensor can simultaneously analyze LPS and HMF. This work provides a new insight for analysis of double targets based on chemoselective ligation assisted DNA walker.

1. Introduction

As versatile and robust building block, DNA has been successfully utilized to construct various artificial molecular machines including DNA walker [1,2], DNA switch [3,4], DNA tweezer [5,6], DNA robot [7,8], and DNA motor [9,10], in view of the exquisite specificity, predictability, and diversity of DNA hybridization. Among them, DNA walker, especially three dimensional (3D) DNA walking nanomachine, is amenable for biosensing due to the relatively high kinetic and processivity [2,11]. It has been proved that the movement of DNA walker on a three-dimensional track can effectively amplify molecular recognition signal [2]. For example, an endonuclease-powered DNA nanomachine can release hundreds of signal probes in response to a single binding event [11].

Currently, the biosensing application of DNA walker focuses on analysis of single target through the introduction of blocker or split strand. [11–17]. Generally, single target cannot well reflect the quality of product and indicate the condition of production. Moreover, the detection of single target can easily lead to false positive result, so it is important to detect multiple targets simultaneously. Compared with single-target assay, multiple-target assay has the advantages including short analytical time, small sample quantity for detection, high analytical efficiency, and low cost.

In this work, chemoselective ligation assisted DNA walker has been constructed and applied as a biosensor to analyze double targets according to the specific output signal combination. On the one hand, chemoselective ligation with high selectivity and superior ligation efficiency as well as mild reaction condition [18–21], will benefit signal input of target and rapid signal conversion. On the other hand, DNA walker owns high processivity so as to ensure the sensitivity of signal output. Moreover, with one-to-one mapping functionality, the developed biosensor can sensitively distinguish all cases of two targets.

2. Experimental section

2.1. Materials and reagents

Lipopolysaccharide (LPS) from *Pseudomonas aeruginosa* 10, streptavidin coated magnetic bead (MB), 5-hydroxymethyl-2-furaldehyde (HMF), pectin, ovalbumin (Ova), alkaline phosphatase (ALP), lactoferrin (LF), glycosylated hemoglobin (GHb), glucose (Glu), galactose (Gal), lactose (Lac), alanine (Ala), and leucine (Leu) were bought from Sigma (Shanghai, China). DNA was synthesized and purified from Sangon Biotech Co., Ltd (Shanghai, China). Nb.BbvC1 (10 units/μL) and Nb.Bts1 (10 units/μL) were purchased from New England Biolabs Inc. (Beijing, China). All other reagents were analytical grade. The deionized water was purified by using a Millipore Milli-Q water purification system (Barnstead, USA) with a resistance value of 18 MΩ cm.

2.2. Construction of chemoselective ligation assisted DNA walker

25 μL Azide modified supporting strand (SSI) (0.48 μM), 25 μL hydroxylamine modified supporting strand (SSII) (0.48 μM), 25 μL carboxyfluorescein (FAM) labelled report strand (RSI) (9.6 μM), and

* Corresponding authors.
E-mail addresses: pengjinhui20110@163.com (J. Peng), juanzhang@shu.edu.cn (J. Zhang).

https://doi.org/10.1016/j.colsurfb.2021.111620
Received 21 December 2020; Received in revised form 30 January 2021; Accepted 5 February 2021
Available online 11 February 2021

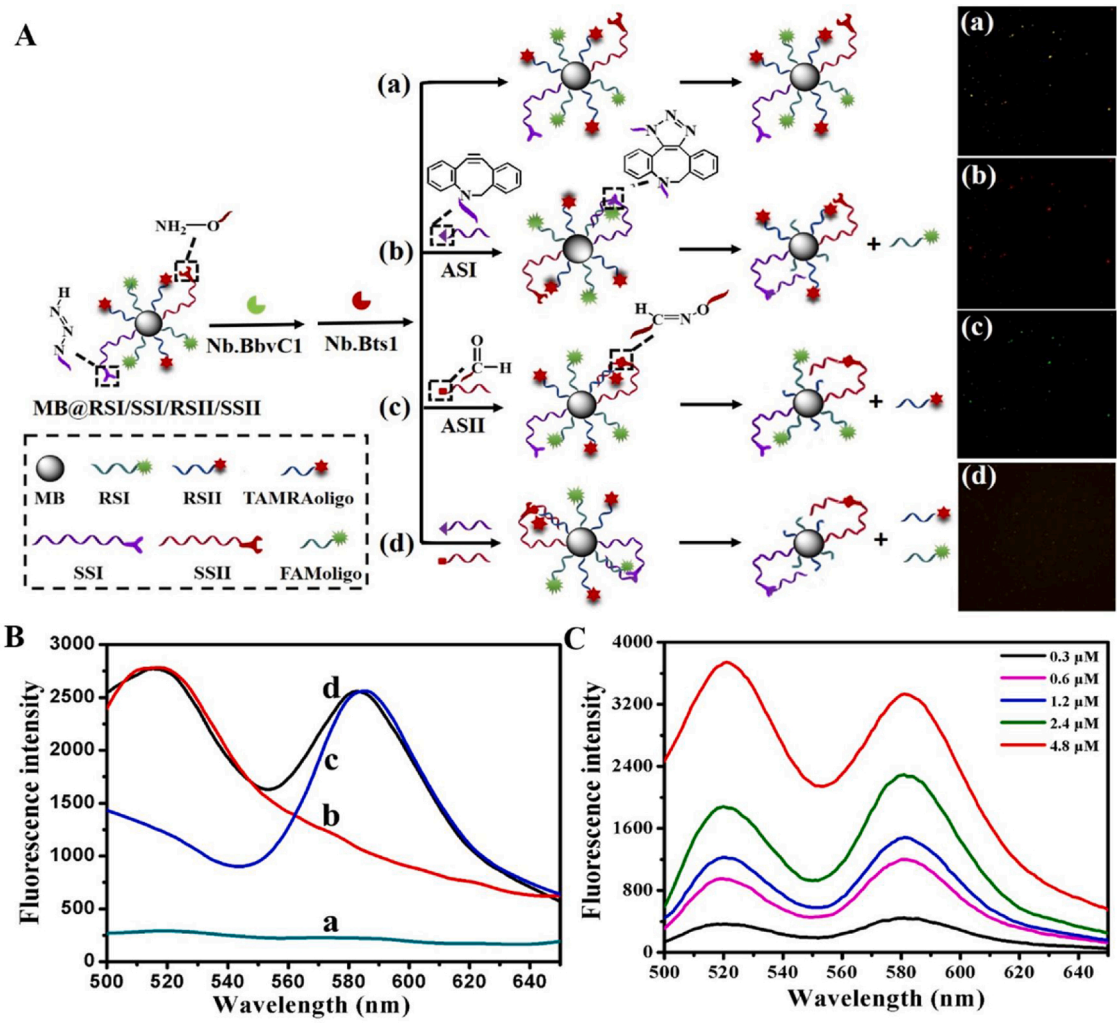

Fig. 1. (A) Schematic illustration of chemoselective ligation assisted DNA walker. The fluorescence images of the modified magnetic beads (a) in absence of both ASI and ASII, (b) in the presence of only ASI, (c) in the presence of only ASII, and (d) in the presence of both ASI and ASII. (B) The fluorescence responses of FAMoligo and TAMRAoligo in the supernatant (a) in absence of both ASI and ASII, (b) in the presence of only ASI, (c) in the presence of only ASII, and (d) in the presence of both ASI and ASII. (C) The fluorescence responses of FAMoligo and TAMRAoligo in the supernatant with simultaneous addition of different concentrations of ASI and ASII at equal molar ratios.

25 μL tetramethyl-6-carboxyrhodamine (TAMRA) labelled report strand (RSII) (9.6 μM) were mixed in phosphate buffer solution (PBS) (10 mM, pH 7.4). Then 100 μL mixing solution was added into 50 μL MB (2 mg/mL) and kept at 30 °C for 1 h, to give MB@RSI/SSI/RSII/SSII after magnetic separation. Subsequently, 50 μL dibenzocyclooctyne (DBCO) modified action strand (ASI) (4.8 μM) and 50 μL aldehyde modified action strand (ASII) (4.8 μM) were mixed with MB@RSI/SSI/RSII/SSII, followed by addition of 2 μL Nb.BbvC1, 2 μL Nb.Bts1, 5 μL cut smart, and 41 μL PBS (10 mM, pH 7.4). The mixture was incubated at 37 °C for 1 h. After magnetic separation, the fluorescence emission spectra of supernatant were tested with 370 nm of excitation wavelength, 10 nm of excitation slit, and 20 nm of emission slit by using fluorescence spectrometer (F-7000, Hitachi Ltd., Japan). The fluorescence images of the modified MB have been acquired through fluorescence microscopy (MF53, Mshot Co. Ltd., China). The measurements were conducted with excitation wavelength of 480 nm and 555 nm for FAM and TAMRA, respectively.

2.3. Comprehensive analysis of LPS and HMF

The mixture of 50 μL LPS aptamer (LPSA) (9.6 μM) and 50 μL ASI (9.6 μM) was heated at 95 °C for 5 min and then cooled naturally, to give LPSA/ASI. Subsequently, 50 μL LPSA/ASI (4.8 μM) and 50 μL ASII (4.8 μM) were added into 50 μL MB@RSI/SSI/RSII/SSII, followed by the addition of different combinations of LPS and HMF including 20 μL LPS (2 ng/mL), 20 μL HMF (1 nM), as well as the mixture of 10 μL LPS (4 ng/mL) and 10 μL HMF (2 nM). After that, 2 μL Nb.BbvC1 and 2 μL Nb.Bts1 were added. The mixture was incubated at 37 °C for 1 h and then separated by magnet. The obtained supernatant was analyzed by using fluorescence spectrometer. In order to fast detect HMF and LPS, fluorescence intensity has been normalized. Generally, LPS with its concentration higher than 1 EU/mL (about 2 ng/mL) [22,23] and HMF with its concentration more than 65.9 mg/kg (about 1 nM) [24] can be found in food product. Therefore, 2 ng/mL LPS and 1 nM HMF have been used to detect FAM and TAMRA fluorescence intensities, respectively, and the fluorescence intensities have been normalized in comparison with that with 10 mg/mL LPS. The acquired normalized fluorescence intensities have been defined as the threshold values.

2.4. Quantitative analysis of LPS

For quantitative analysis of LPS, 50 μL LPSA (9.6 μM) was mixed with 50 μL ASI (9.6 μM) at 37 °C for 2 h, to give LPSA/ASI. Subsequently, 100 μL LPS with different concentrations was mixed with 50 μL

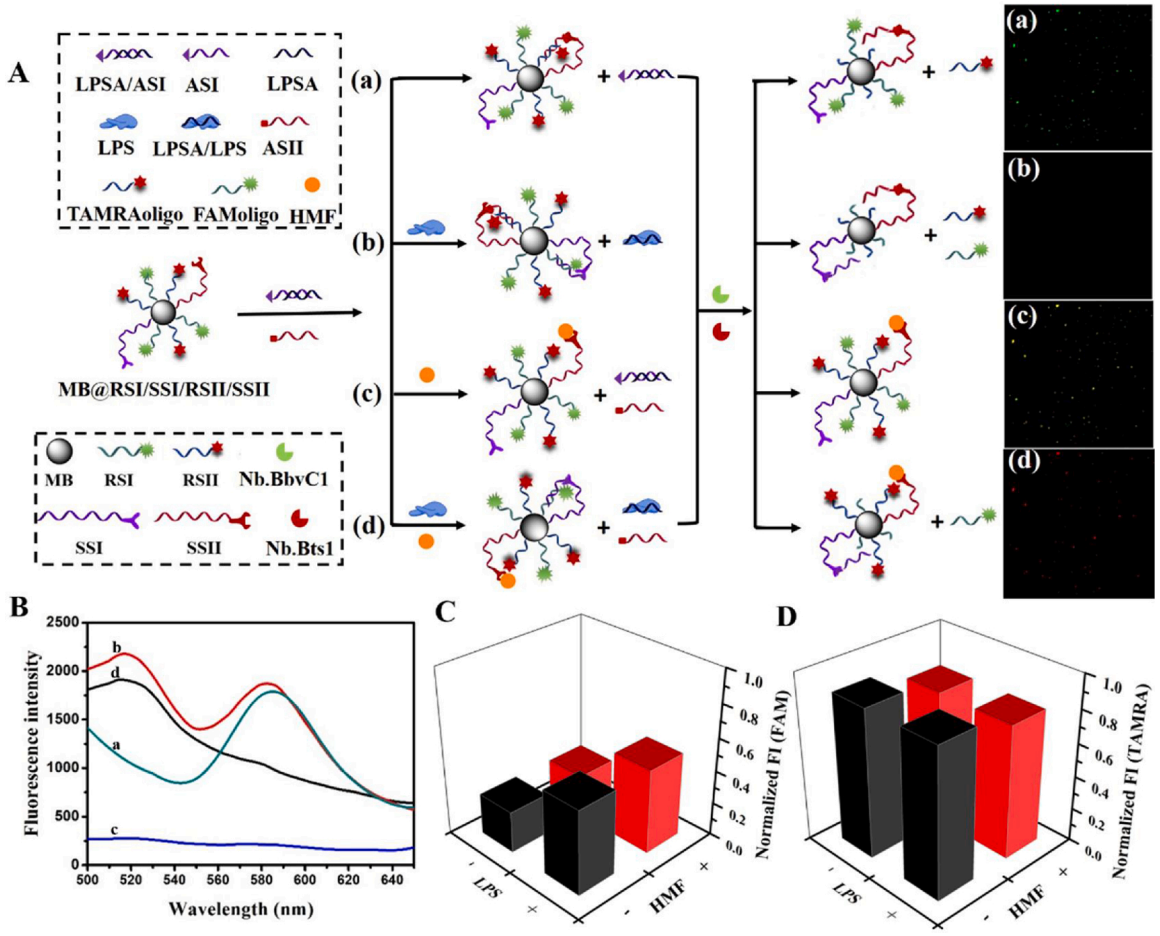

Fig. 2. (A) Schematic illustration of analysis of double targets based on chemoselective ligation assisted DNA walker. The fluorescence images of the modified MB (a) in absence of both LPS and HMF, (b) in the presence of only LPS, (c) in the presence of only HMF, and (d) in the presence of both LPS and HMF. (B) The fluorescence responses of FAMoligo and TAMRAoligo in the supernatant (a) in absence of both LPS and HMF, (b) in the presence of only LPS, (c) in the presence of only HMF, and (d) in the presence of both LPS and HMF. (C) Normalized fluorescence intensities of FAMoligo against different combinations of LPS and HMF. (D) Normalized fluorescence intensities of TAMRAoligo against different combinations of LPS and HMF.

LPSA/ASI (4.8 μM), 50 μL ASII (4.8 μM), and 50 μL MB@RSI/SSI/RSII/SSII, followed by the addition of 2 μL Nb.BbvC1, 2 μL Nb.Bts1, 5 μL cut smart, and 41 μL PBS (10 mM, pH 7.4). The mixture was incubated at 37 °C for 1 h. After magnetic separation, the fluorescence emission spectra of supernatant were determined. The emission spectra were recorded from 500 nm to 650 nm with excitation wavelength of 370 nm. The excitation slit was 10 nm. The emission slit was 20 nm. The photomultiplier voltage was 900 V.

2.5. Quantitative analysis of HMF

100 μL HMF with different concentrations was mixed with 50 μL ASII (4.8 μM), 50 μL LPSA/ASI (4.8 μM), 50 μL MB@RSI/SSI/RSII/SSII, 2 μL Nb.BbvC1, 2 μL Nb.Bts1, 5 μL cut smart, and 41 μL PBS (10 mM, pH 7.4). Then, the mixture was kept at 37 °C for 1 h. The obtained supernatant after magnetic separation was utilized for determination of fluorescence emission spectra. The emission spectra were recorded from 500 nm to 650 nm with excitation wavelength of 370 nm. The excitation slit was 10 nm. The emission slit was 20 nm. The photomultiplier voltage was 900 V.

3. Results and discussion

3.1. Chemoselective ligation assisted DNA walker

Fig. 1(A) shows the operation principle of chemoselective ligation assisted DNA walker. In absence of both ASI and ASII, there is no fluorescence observed in the supernatant after magnetic separation ((a), Fig. 1(A)). The added ASI can covalently conjugate with SSI through cycloaddition reaction, followed by self-assembly of ASI and RSI to form the double strand through complementary base pairing. Nb.BbvC1 can specifically cut down the formed double strand, resulting in the release of FAM-labeled oligonucleotide (FAMoligo) from the surface of MB into the solution, causing the occurrence of FAM fluorescence in the supernatant ((b), Fig. 1(A)). Similarly, the added ASII can lead to the linkage between ASII and SSII via oxime chemistry and the following dissociation of TAMRA-labeled oligonucleotide (TAMRAoligo) cleaved by Nb.Bts1 as well as the happening of TAMRA fluorescence in the supernatant ((c), Fig. 1(A)). In the coexistence of both ASI and ASII, FAMoligo and TAMRAoligo can be simultaneously released from the surface of modified MB after magnetic separation, leading to simultaneous occurrence of FAM and TAMRA fluorescences in the supernatant ((d), Fig. 1(A)).

Chemoselective ligation assisted DNA walker has been investigated by detecting the fluorescence intensities of FAM and TAMRA. In absence of both ASI and ASII, the fluorescence can be found for the modified MB (Image a, Fig. 1(A)), and no fluorescence peak in the supernatant can be

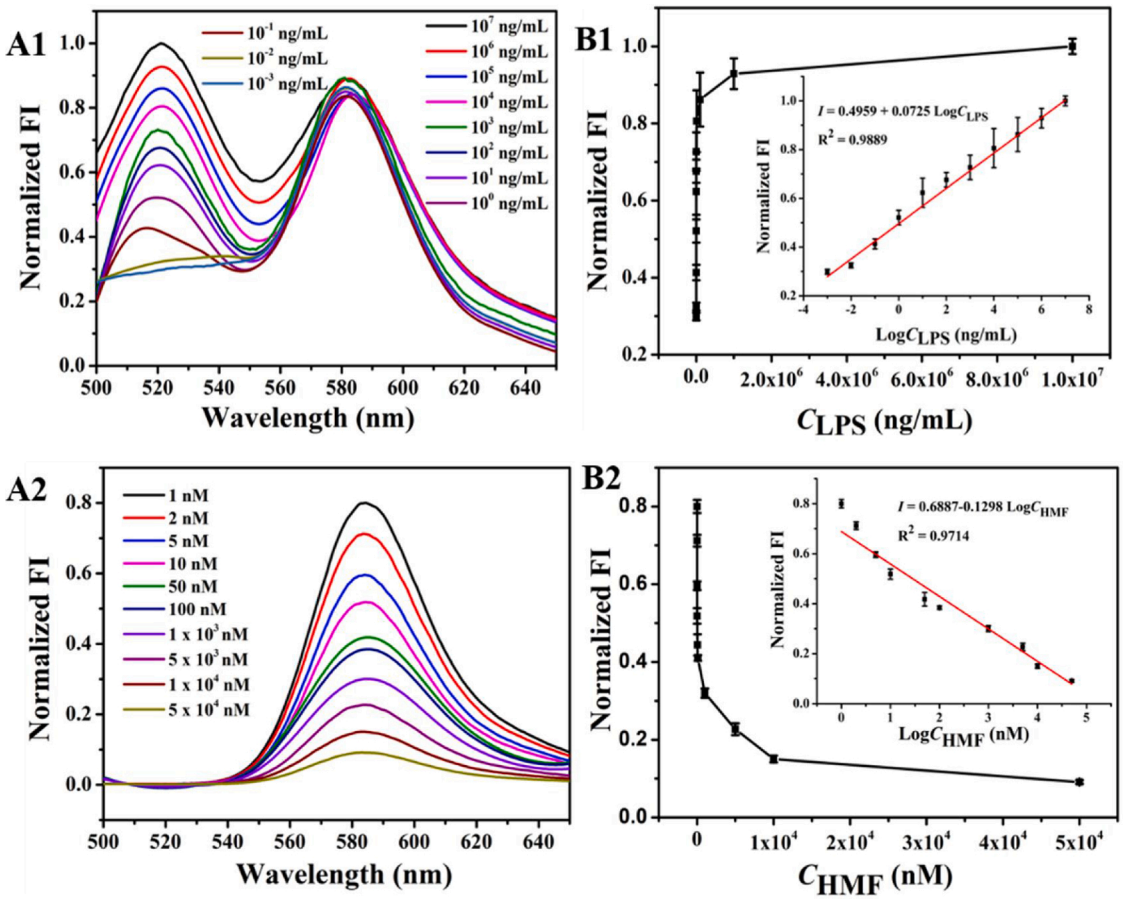

Fig. 3. Fluorescence spectra upon adding different concentrations of (A1) LPS and (A2) HMF. The normalized fluorescence intensities at (B1) 522 nm and (B2) 584 nm against the concentrations of LPS and HMF, respectively. Inset: linear relationship between the normalized intensities and logarithmic values of target concentrations.

found (Curve a, Fig. 1(B)). In the presence of only ASI, the bright red fluorescence can be observed for the modified MB (Image b, Fig. 1(A)) and high FAM fluorescence signal value at 522 nm can be given for the supernatant (Curve b, Fig. 1(B)). It can be explained for the reason that ASI can link with SSI through cycloaddition reaction, accompanying the self-assembly of double strand and the subsequent release of FAMoligo cleaved by nicking endonuclease Nb.BbvC1. In the presence of only ASII, green fluorescence can be found for the modified MB (Image c, Fig. 1(A)) and the TAMRA fluorescence peak at 584 nm appears for the supernatant (Curve c, Fig. 1(B)). It can be ascribed for the fact that ASII can coordinate with SSII via oxime chemistry, followed by cleavage of TAMRAoligo by nicking endonuclease Nb.Bts1 and its removal from surface of modified MB into the supernatant. In the presence of both ASI and ASII, almost no fluorescence can be observed for the modified MB (Image d, Fig. 1(A)) and two peaks emerge in the supernatant (Curve d, Fig. 1(B)). ASI and ASII can separately conjugate with SSI and SSII through cycloaddition reaction and oxime reaction, resulting in the disappearance of red and green fluorescences for the modified MB and coinstantaneous occurrence of FAMoligo and TAMRAoligo in the supernatant.

To achieve highest efficiency for simultaneous performance of cycloaddition reaction and oxime chemistry, the experimental conditions have been optimized, and the optimal time and pH value obtained are 1 h and 7.4, respectively (Fig. S1 (A) and (B)). Under optimal conditions, different concentrations of ASI and ASII at equal molar ratios have been added into the reaction system and the fluorescence intensities of supernatant have been detected (Fig. 1(C)). It can be found that the fluorescence intensities gradually increase with the increasing concentrations of both ASI and ASII from 0.3 μM to 4.8 μM. The results well confirm that chemoselective ligation assisted DNA walker can be exploited as a biosensor with double signal inputs and outputs.

3.2. Investigation of mechanism for analysis of double targets

Fig. 2(A) shows the principle of analysis of double targets. Herein, the mixture containing MB@RSI/SSI/RSII/SSII, LPSA/ASI, and ASII, can be utilized as preliminary platform for output of high or low signal. In the initial state, only red fluorescence can be observed in the supernatant after magnetic separation ((a), Fig. 2(A)), resulting from the formation of oxime bond and subsequent cleavage of self-assembled double strand by nicking endonuclease Nb.Bts1. Through target-induced strand release, the added LPS can lead to the dissociation of ASI from LPSA/ASI and the released ASI can covalently conjugate with SSI through cycloaddition reaction, resulting in the release of FAMoligo from the surface of MB into the solution. So in the presence of only LPS, green and red fluorescence will occur simultaneously in the supernatant ((b), Fig. 2 (A)). Moreover, the added HMF can competitively react with ASII to produce oxime bond so as to inhibit the covalent linkage between ASII and SSII and eventual dissociation of TAMRAoligo. So almost no fluorescence can be found in the supernatant ((c), Fig. 2(A)). In the coexistence of both LPS and HMF, only FAMoligo can be released into the supernatant after magnetic separation ((d), Fig. 2(A)).

The analysis of double targets has been investigated by detecting the fluorescence intensity of FAM and TAMRA. In absence of any target, bright green fluorescence can be given for the modified MB (Image a, Fig. 2(A)) and only fluorescence signal at 584 nm can be found in the supernatant (Curve a, Fig. 2(B)). ASII can covalently link onto the surface of modified MB through the formation of oxime bond,

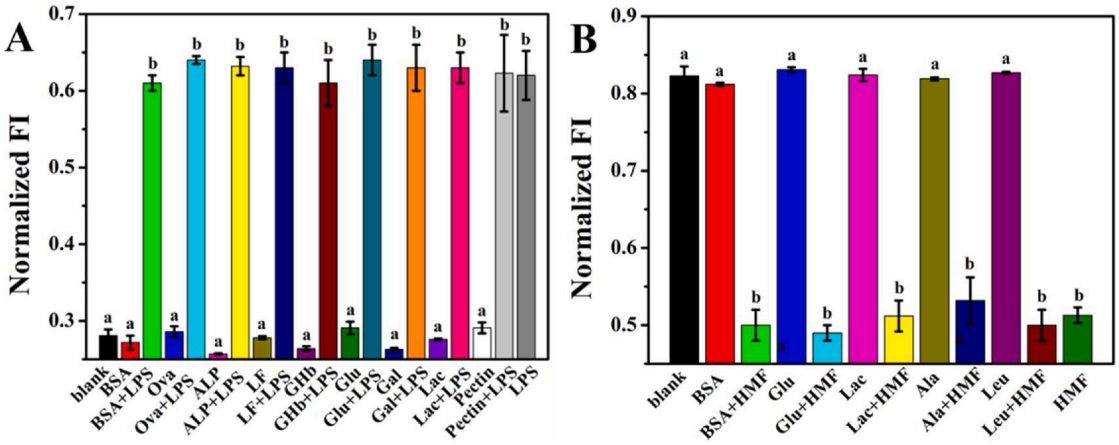

Fig. 4. (A) Specificity of chemoselective ligation assisted DNA walker for LPS analysis against blank, BSA (1 μg/mL), BSA (1 μg/mL) + LPS (10 ng/mL), Ova (1 μg/mL), Ova (1 μg/mL) + LPS (10 ng/mL), ALP (1 μg/mL), ALP (1 μg/mL) + LPS (10 ng/mL), LF (1 μg/mL), LF (1 μg/mL) + LPS (10 ng/mL), GHb (1 μg/mL), GHb (1 μg/mL) + LPS (10 ng/mL), Glu (1 μg/mL), Glu (1 μg/mL) + LPS (10 ng/mL), Gal (1 μg/mL), Gal (1 μg/mL) + LPS (10 ng/mL), Lac (1 μg/mL), Lac (1 μg/mL) + LPS (10 ng/mL), Pectin (1 μg/mL), Pectin (1 μg/mL) + LPS (10 ng/mL), and LPS (10 ng/mL). (B) Specificity of chemoselective ligation assisted DNA walker for HMF analysis against blank, BSA (1 μM), BSA (1 μM) + HMF (10 nM), Glu (1 μM), Glu (1 μM) + HMF (10 nM), Lac (1 μM), Lac (1 μM) + HMF (10 nM), Ala (1 μM), Ala (1 μM) + HMF (10 nM), Leu (1 μM), Leu (1 μM) + HMF (10 nM), and HMF (10 nM). Columns labeled by different letters indicate significant statistical diff ; erentiation ($p \leq 0.05$).

accompanying self-assembly of double strand and subsequent release of TAMRAoligo. With LPS, almost no fluorescence can be observed for the modified MB (Image b, Fig. 2(A)) and high fluorescence signal values at 522 nm and 584 nm can be given (Curve b, Fig. 2(B)). LPS can induce the release of ASI which can link with SSI through cycloaddition reaction, accompanying the self-assembly of double strand and the subsequent release of FAMoligo cleaved by nicking endonuclease Nb.BbvC1. In the presence of only HMF, green and red fluorescences for modified MB can be seen (Image c, Fig. 2(C)) and almost no fluorescence peak can be observed for the supernatant (Curve c, Fig. 2(B)). On the one hand, HMF can prevent the coordination between ASII with SSII and corresponding cleavage of TAMRAoligo. On the other hand, ASI cannot covalently bind onto the surface of MB due to the preventing effect of LPSA. Moreover, strong red fluorescence for modified MB and high value of fluorescence peak at 522 nm can be observed with both LPS and HMF (Image d, Fig. 2(A); Curve d, Fig. 2(B)). It can be attributed for the promotion effect of LPS on the release of FAMoligo and the prevention effect of HMF on the release of TAMRAoligo from the surface of modified MB into the supernatant.

Under optimized conditions (Fig. S1), fluorescence intensities have been normalized to analyze LPS and HMF. Fig. 2(C) and (D) separately give the column bars of the fluorescence intensities of FAMoligo at 522 nm and TAMRAoligo at 584 nm against the input combinations of LPS and HMF. If FAMoligo intensity is lower than 0.25 and TAMRAoligo intensity higher than 0.89, it implies neither LPS nor HMF existing in the sample. If FAMoligo fluorescence intensity is higher than 0.51 and TAMRAoligo intensity higher than 0.89, it indicates the appearance of only LPS in the sample. If FAMoligo intensity is lower than 0.25 and TAMRAoligo intensity lower than 0.8, it suggests the existence of only HMF in the sample. If FAMoligo intensity is higher than 0.51 and TAMRAoligo intensity lower than 0.8, it suggests the simultaneous occurrence of both LPS and HMF in the sample system. Therefore, the whole set of combinations of LPS and HMF can be fast characterized without the loss of any information.

3.3. Quantitative analysis of double targets

Double targets including LPS and HMF are quantitatively analyzed by using chemoselective ligation assisted DNA walker. As shown in Fig. 3(A1), along with the increased concentrations of LPS from 10^{-3} ng/mL to 10^{7}ng/mL, the fluorescence intensities gradually increase. It can be ascribed for the increasing release of ASI induced by LPS and the following removal of FAMoligo from the surface of MB. LPS can competitively combine with its aptamer, resulting in the release of ASI from hybridized LPSA/ASI. Subsequently, the released AS can enter DNA walking reaction system and be immobilized onto the surface of MB through its hydrazone reaction with SSI, so as to trigger the performance of DNA walker along spherical nucleic acid track and the departure of fluorescence probe into the solution. The steric effect occurring with the formation of LPSA/ASI can not only inhibit chemoselective ligation reaction but also prevent the cleavage of RSI catalyze by nicking enzyme. The fluorescence intensities linearly increase with logarithmic values of LPS concentrations from 10^{-3} ng/mL to 10^{7} ng/mL (Inset, Fig. 3(B1)), which is wider than the previous reports [25,26]. The lowest detection limit has been calculated to be 0.008 ng/mL, through interpolation of three times standard deviation of six blank measurements, and the value is lower than the reports [25,27,28]. Meanwhile, 5.67 % of relative standard deviation (RSD) values have been obtained by using the slopes of three regression equation to evaluate detection precision. Different from LPS, HMF can result in the decrease of the fluorescence intensities with its increasing concentrations (Fig. 3(A2)). It can be explained for the formation of oxime bond which inhibits the performance of DNA walker and the release of TAMRAoligo. Moreover, it can be found that the fluorescence intensities linearly reduce with the increased logarithmic values of HMF concentrations from 1 nM to 5×10^{4} nM. The linear fitting equation of $I = 0.6887 - 0.1298\ \mathrm{Log}C$ can be obtained with the detection limit of 0.8 nM, lower than the previous reports [29–31]. Furthermore, RSD values can be calculated to be 3.94 %. These results well confirm the good reproducibility and precision of chemoselective ligation assisted DNA walker.

3.4. Investigation for specificity of chemoselective ligation assisted DNA walker

For the investigation for the specificity of chemoselective ligation assisted DNA walker for LPS analysis, the interfering substances including protein (BSA), glycoproteins (Ova, ALP, LF, and GHb), monosaccharides (Glu and Gal), oligosaccharide (Lac), and polysaccharide (pectin), with 100 times high concentration than that of LPS have been selected (Fig. 4(A)). The high normalized fluorescence intensities can be detected for LPS and its mixtures with interfering substances. It signifies that the interfering substances have no impact on the

Table 1
The concentrations detected and the comparison with the given concentrations in soft drinks samples.

	Sample	The concentration detected	Standard concentration	Recovery ratio (%)	Relative error (%)
LPS	Orange juice	1 1.016×10 ng/mL	10 ng/mL	101.60	1.8
		2 1.039 ng/mL	1 ng/mL	103.90	1.6
		3 0.976×10^{-1} ng/mL	10^{-1} ng/mL	97.60	2.6
		4 0.963×10^{-2} ng/mL	10^{-2} ng/mL	96.26	2.8
	Black tea	1 1.021×10 ng/mL	10 ng/mL	102.07	3.5
		2 1.041 ng/mL	1 ng/mL	104.11	3.7
		3 0.976×10^{-1} ng/mL	10^{-1} ng/mL	97.60	1.9
		4 1.035×10^{-2} ng/mL	10^{-2} ng/mL	103.50	2.5
	Milk	1 1.031×10 ng/mL	10 ng/mL	103.06	1.6
		2 1.047 ng/mL	1 ng/mL	104.70	3.6
		3 0.973×10^{-1} ng/mL	10^{-1} ng/mL	97.30	2.7
		4 0.955×10^{-2} ng/mL	10^{-2} ng/mL	95.54	3.0
HMF	Orange juice	1 10.230 nM	10 nM	102.30	5.6
		2 4.961 nM	5 nM	99.22	4.3
		3 2.046 nM	2 nM	102.30	2.9
		4 0.968 nM	1 nM	96.80	6.3
	Black tea	1 10.960 nM	10 nM	109.60	8.1
		2 5.236 nM	5 nM	104.72	5.9
		3 1.865 nM	2 nM	93.25	4.1
		4 0.963 nM	1 nM	96.30	7.6
	Milk	1 10.350 nM	10 nM	103.50	7.3
		2 4.863 nM	5 nM	97.26	2.6
		3 1.924 nM	2 nM	96.20	5.1
		4 0.918 nM	1 nM	91.80	5.4

release of ASI from hybridized double strand induced by the binding of LPS. In contrast, all interfering substances show low values of normalized fluorescence intensities. It well proves that these substances cannot induce the release of ASI from hybridized double strand LPSA/ASI. These results confirm the high specificity of the established method based on chemoselective ligation assisted DNA walker for LPS analysis. It can be attributed for high specificity of aptamer to bind with LPS.

To investigate the specificity of chemoselective ligation assisted DNA walker for HMF analysis, protein (BSA), monosaccharide (Glu), disaccharide (Lac), and amino acids (Ala and Leu) have been selected as interfering substances and the corresponding results have been shown in Fig. 4(B). HMF and its mixture with the interfering substances exhibit low values of normalized fluorescence intensities. It suggests that these substances have no influence on oxime reaction between HMF and SSII and the following analysis of HMF. On the contrary, high normalized fluorescence intensities can be found for the interfering substances. The results well confirm that these substances have nearly no impact on the occurrence of oxime reaction between ASII and SSII. These results well suggest that the established method owns high specificity for the detection of HMF. It can be explained for the specificity of oxime linkage.

3.5. Analysis of real sample through chemoselective ligation assisted DNA walker

We further use chemoselective ligation assisted DNA walker to analyze the spiked sample and the corresponding results have been exhibited in Table 1. The recovery ratio varies from 91.80 % to 109.60 %, and the relative errors are within 9 %. These results well suggest that chemoselective ligation assisted DNA walker can be well utilized for simultaneous analysis of double targets in the real samples.

4. Conclusions

In summary, chemoselective ligation assisted DNA walker has been designed for input and output of double signals and further been utilized as a biosensor with LPS and HMF as the two inputs. The one-to-one mapping function of the biosensor endows it capability to differentiate all original input patterns including the absence of both LPS and HMF, the presence of only LPS, the presence of only HMF, and the presence of both LPS and HMF from the corresponding outputs, so as to realize rapid analysis of LPS and HMF. Moreover, the biosensor shows wide linear range, low detection limit, high specificity, as well as good reproducibility and practicability.

CRediT authorship contribution statement

Tianxiang Xue: Methodology, Conceptualization, Writing - original draft. **Longfei Tang:** Investigation, Resources. **Xiquan Yue:** Investigation, Visualization, Supervision. **Lili Niu:** Investigation, Data curation. **Jinhui Peng:** Investigation, Formal analysis. **Juan Zhang:** Funding acquisition, Writing - review & editing.

Declaration of Competing Interest

The authors declare that they have no known competing financial interests or personal relationships that could have appeared to influence the work reported in this paper.

Acknowledgements

This work is sponsored by the National Natural Science Foundation of China (Grant No. 31671923), and Science and Technology Commission of Shanghai Municipality (Grant Nos. 20392001800, 20Y11912700 and 18PJD016).

Appendix A. Supplementary data

Supplementary material related to this article can be found, in the online version, at doi:https://doi.org/10.1016/j.colsurfb.2021.111620.

References

[1] J.S. Shin, N.A. Pierce, A synthetic DNA walker for molecular transport, Am. Chem. Soc. 126 (2004) 10834–10835.
[2] X. Qu, D. Zhu, G. Yao, S. Su, J. Chao, H. Liu, An exonuclease III-powered, on-particle stochastic DNA walker, Angew. Chem. 56 (2017) 1855–1858.
[3] F. Wang, X. Liu, I. Willner, DNA switches: from principles to applications, Angew. Chem., Int. Ed. 54 (2015) 1098–1129.
[4] F. Wang, X. Liu, I. Willner, DNA-schalter: grundlagen and anwendungen, Angew. Chem. 127 (2015) 1112–1144.
[5] M. Liu, J. Fu, C. Hejesen, Y. Yang, N.W. Woodbury, K. Gothelf, A DNA tweezer-actuated enzyme nanoreactor, Nat. Commun. 4 (2013), 2127-2127.
[6] C. Zhou, Z. Yang, D. Liu, Reversible regulation of protein binding affinity by a DNA machine, J. Am. Chem. Soc. 134 (2012) 1416–1418.
[7] K. Lund, A.J. Manzo, N. Dabby, N. Michelotti, A. Johnson-Buck, J. Nangreave, Molecular robots guided by prescriptive landscapes, Nature 465 (2010), 206-206.
[8] Y. Amir, E. Ben-Ishay, D. Levner, S. Ittah, A. Abu-Horowitz, I. Bachelet, Universal computing by DNA origami robots in a living animal, Nat. Commun. 9 (2014), 353-353.
[9] T.G. Cha, J. Pan, H. Chen, J. Salgado, X. Li, C. Mao, A synthetic DNA motor that transports nanoparticles along carbon nanotubes, Nat. Nanotechnol. 9 (2013), 39-39.
[10] M. Liber, T.E. Tomov, R. Tsukanov, Y. Berger, E. Nir, A bipedal DNA motor that travels back and forth between two DNA Origami Tiles, Small 11 (2015) 568–575.
[11] X. Yang, Y. Tang, S.D. Mason, J. Chen, F. Li, Enzyme-powered three-dimensional DNA nanomachine for DNA walking, payload release, and biosensing, ACS Nano 10 (2016) 2324–2330.
[12] C. Feng, Z.H. Wang, T.S. Chen, X.X. Chen, D.S. Mao, J. Zhao, A dual-enzyme-assisted three-dimensional DNA walking machine using T4 polynucleotide kinase

as activators and application in polynucleotide kinase assays, Anal. Chem. 90 (2018) 2810–2815.
[13] Y. Li, G.A. Wang, S.D. Mason, X. Yang, Z. Yu, Y. Tang, Simulation-guided engineering of an enzyme-powered three dimensional DNA nanomachine for discriminating single nucleotide variants, Chem. Sci. 9 (2018) 6434–6439.
[14] H. Zhang, M. Lai, A. Zuehlke, H. Peng, X.F. Li, X.C. Le, Binding-induced DNA nanomachines triggered by proteins and nucleic acids, Angew. Chem. 54 (2015) 14326–14330.
[15] W. Li, L. Wang, W. Jiang, A catalytic assembled enzyme-free three-dimensional DNA walker and its sensing application, Chem. Commun. 53 (2017), 5527-5230.
[16] M. Qing, S. Xie, W. Cai, D. Tang, Y. Tang, J. Zhang, Click chemistry reaction-triggered 3D DNA walking machine forsensitive electrochemical detection of copper Ion, Anal. Chem. 90 (2018) 11439–11445.
[17] J. Zhang, X. Wang, T. Chen, C. Feng, G. Li, Electrochemical analysis of enzyme based on the self-a ssembly of lipid bilayer on an electrode surface mediated by hydrazone chemistry, Anal. Chem. 89 (2017) 13245–13251.
[18] P.V. Robinson, G. de Almeida-Escobedo, A.E. de Groot, J.L. McKechnie, C. R. Bertozzi, Live-cell labeling of specific protein glycoforms by proximity-enhanced bioorthogonal ligation, J. Am. Chem. Soc. 137 (2015) 10452–10455.
[19] A. Mukhortava, M. Schlierf, Efficient formation of site-specific protein-DNA hybrids using copper-free click chemistry, Bioconjugate Chem. 27 (2016) 1559–1563.
[20] Y. Xiong, X. Li, M. Li, H. Qin, C. Chen, D. Wang, What is hidden behind schiff base hydrolysis dynamic covalent chemistry for the precise capture of sialylated glycans, Am. Chem. Soc. 142 (2020) 7627–7637.
[21] Melanie R. Rutkowski, Tom L. Stephen, N. Svoronos, Michael J. Allegrezza, Amelia J. Tesone, A. Perales-Puchalt, Microbially driven TLR5-dependent signaling governs distal malignant progression through tumor-promoting inflammation, Cancer Cell 27 (2015) 27–40.
[22] T.M. Wassenaar, K. Zimmermann, Lipopolysaccharides in food, food supplements, and probiotics: should we be worried, Eur. J. Microbiol. Immunol. 8 (2018) 63–69.
[23] J.H. van den Berg, S.G. Quaak, J.H. Beijnen, W.E. Hennink, G. Storm, T. N. Schumacher, Lipopolysaccharide contamination in intradermal DNA vaccination: toxic impurity or adjuvant, Int. J. Pharm. 390 (2010) 32–36.
[24] S. Kowalski, M. Lukasiewicz, A. Duda-Chodak, G. Zięć, 5-Hydroxymethyl-2-Furfural (HMF)-Heat-induced formation, occurrence in food and biotransformation-a Review, Pol. J. Food Nutr. Sci. 63 (2013) 207–225.
[25] P.Y. Xie, L.J. Zhu, X.L. Shao, K.L. Huang, J.J. Tian, W.T. Xu, Highly sensitive detection of lipopolysaccharides using an aptasensor based on hybridization chain reaction, Sci. Rep. 6 (2016), 29524-29524.
[26] W.J. Shen, Y. Zhuo, Y.Q. Chai, R. Yuan, Cu-based metal-organic frameworks as a catalyst to construct a ratiometric electrochemical aptasensor for sensitive lipopolysaccharide detection, Anal. Chem. 87 (2015) 11345–11352.
[27] S.J. Ding, B.W. Chang, C.C. Wu, C.J. Chen, H.C. Chang, A new method for detection of endotoxin on polymyxin B-immobilized gold electrodes, Electrochem. Commun. 9 (2007) 1206–1211.
[28] G. Priano, D. Pallarola, F. Battaglini, Endotoxin detection in a competitive electrochemical assay: synthesis of a suitable endotoxin conjugate, Anal. Biochem. 362 (2007) 108–116.
[29] Y. Guan, X. Wu, H. Meng, Indirect competitive ELISA based on monoclonal antibody for the detection of 5-hydroxymethyl-2-furfural in milk, compared with HPLC, J. Dairy Sci. 96 (2013) 4885–4890.
[30] J.K. de Andrade, E. Komatsu, H. Perreault, Y.R. Torres, M.R. da Rosa, M.L. Felsner, In house validation from direct determination of 5-hydroxymethyl-2-furfural (HMF) in Brazilian corn and cane syrups samples by HPLC-UV, Food Chem. 190 (2016) 481–486.
[31] J.K. de Andrade, C.K. de Andrade, E. Komatsu, H. Perreault, Y.R. Torres, M.R. da Rosa, A validated fast difference spectrophotometric method for 5-hydroxymethyl-2-furfural (HMF) determination in corn syrups, Food Chem. 228 (2017) 197–203.